Synthesis and Evaluation of *N*-Benzyl-Acridinone Derivatives Induced Apoptosis in Human Liver Cancer Cell-Lines

Xian-Feng Huang*[,a], Yulan-Zhu[a] and Hai-Liang Zhu*[,b]

[a]*School of Pharmaceutical Engineering & Life Science, Changzhou University, Changzhou, 213164, P.R. China*

[b]*State Key Laboratory of Pharmaceutical Biotechnology, Nanjing University, Nanjing 210093, P.R. China*

Received February 14, 2011: Revised May 13, 2011: Accepted May 16, 2011

Abstract: A series of *N*-benzyl-9(10*H*)-acridinones were synthesized and tested for their antitumor activities *in vitro* against HepG2 cells. Assay-based antiproliferative activity study using HepG2 cell lines revealed that several compounds had significant effects on cytotoxicity, among which compound **5h** was found to be the most active compound with IC_{50} at about 1.33 μM using the MTT assay. The antitumor effect of compound **5h** is believed to be due to the induction of apoptosis, which was further confirmed by Hoechst 33258 fluorescence staining, agarose gel electrophoresis and Annexin V-FITC/PI staining assay using flow cytometry analysis. Above all, compound **5h** would be a potential anticancer agent which deserves further research.

Keywords: Acridinone, Antiproliferative activity, Apoptosis, HepG2 cell.

1. INTRODUCTION

Hepatocellular carcinoma (HCC) is one of the most common cancers worldwide, with a particularly high prevalence in Asian countries, due to endemic hepatitis B virus (HBV) infection [1-4]. HCC is a rapidly fatal disease and HCC patients have caused cirrhosis and impaired liver function, making treatment of HCC more difficult than many other cancers [5, 6]. The survival of cancer cells depends on their ability to adapt changes in their microenvironment and to escape from the growth-inhibitory effects of neighboring normal cells and to resist apoptosis and growth-inhibitory signals, leading to tissue invasion and metastasis. The regulation of apoptosis is crucial for development and sustained health [7-9]. The dysregulation of apoptosis will result in a variety of clinical disorders including cancer. Most chemotherapeutic agents used in cancer therapy kill particular types of tumor cells through apoptosis and do not damage organism. Therefore, anticancer drugs killing tumor cells through apoptosis have been widely studied in medicinal chemistry [10-13].

Acridone derivatives have been known for many years as antimicrobial agents [14]. The planar, heterocyclic and considerably hydrophobic nature of acridone, making it to interact with several biomolecular targets, led to the investigations of a number of acridone derivatives for their anti-tumor [15-18], anti-protozoan [19-21] and anti-viral [22] properties. Recently, several research groups have reported a series of 10-benzyl-9(10*H*)-acridinones and their *in vitro* antitumor activities against various cell lines [23, 24].

In this paper, we describe the synthesis, SAR, and antitumor effects of a series of 10-benzyl-9(10*H*)-acridinone derivatives including some new compounds and reported ones on one human liver carcinoma cell line (Hep G2) *in vitro*. The activity has also been confirmed by Hoechst 33258 fluorescence staining, agarose gel electrophoresis and Annexin V-FITC/PI staining assay using flow cytometry analysis.

2. CHEMISTRY

Acridone derivatives **5a-5j** variously functionalized at the C-ring were synthesized as reported [25] in Scheme 1. We first synthesized *N*-(carboxyphenyl) anthranilic acid (**3**) on a preparative scale, using the method of Jourdan–Ulmann copper-catalyzed condensation of o-chlorobenzoic acid and 4-chloroaniline. The reactants were heated preferably at reflux in the presence of copper powder and K_2CO_3 in DMF medium. The *N*-(carboxyphenyl) anthranilic acids were cyclized with polyphosphoric acid at 120 ^oC to form variously functionalized acridones (**4**). Following this methodology, we prepared a series of *N*-benzyl-9(10H)-acridinones. Then target compounds were obtained by N^{10}-alkylation by corresponding benzyl chloride and K_2CO_3 in DMF. All compounds were fully characterized by ^1H NMR, ESI MS and elemental analysis. The structure of compound **5d** was also established by X-ray crystallographic analysis (Fig. **1**). Of all the compounds, **5d**, **5f**, **5h** and **5j** were new compounds and others have been reported [26, 27].

3. CYTOTOXICITY MEASUREMENT

In vitro cytotoxic activities of these *N*-Substituted acridones were studied on a panel of one human liver carcinoma cell line (Hep G2). All of the compounds displayed potent cytotoxic activities against Hep G2. The cytotoxic activity of the 10 compounds in Hep G2 was closely associated with their structures, as shown in Table **1** and expressed as the half maximal inhibitory concentration (IC_{50}).

*Address correspondence to these authors at the School of Pharmaceutical Engineering & Life Science, Changzhou University, Changzhou, 213164, P. R. China; Tel: +86-519-8633 0167; Fax: +86-25-8633 0167;
E-mail: xianfenghh@163.com
State Key Laboratory of Pharmaceutical Biotechnology, Nanjing University, Nanjing 210093, P. R. China; Tel: +86-25-8359 2572; Fax: +86-25-8359 2672; E-mail: zhuhl@nju.edu.cn

1570-1808/11 $58.00+.00

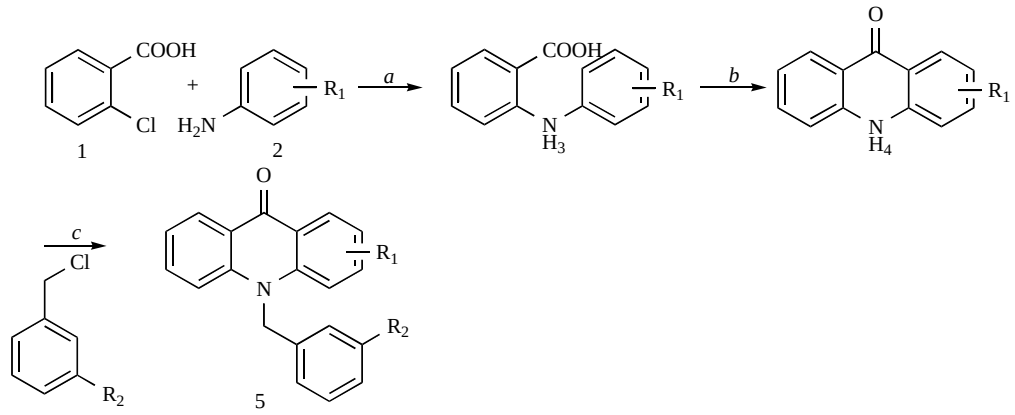

Scheme 1. Synthesis of compounds **5a**–**5j**. Reagents and conditions: (a) K_2CO_3, Cu, DMF, rt, 6 h; (b) PPA, 120 °C, 3 h; (c) K_2CO_3, DMF, 90-100 °C, 3-6 h.

Out of the 10 compounds, 5 compounds exhibited good activity with IC_{50} values of <6.0 μM, among which 3 compounds (**5d**, **5g**, **5h**) demonstrated IC_{50} values of 1.0-3.0 μM, compound **5h** exhibited the most potential inhibitory activity in tumor growth inhibition (IC_{50}=1.33 μM), being better than that of 5-Fu.

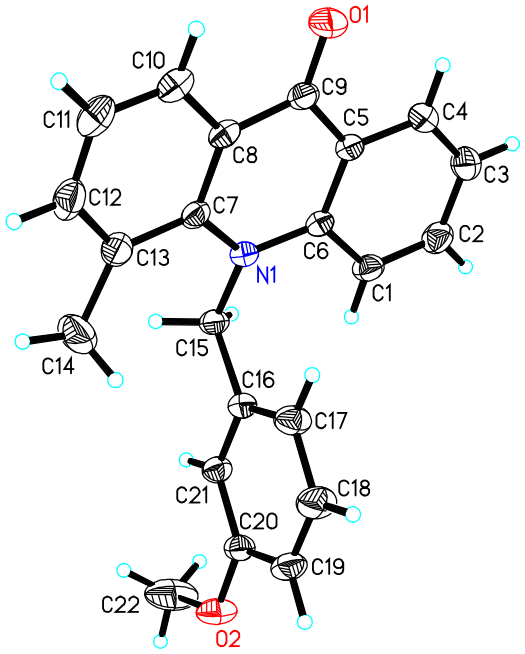

Fig. (1). Crystal structure of the compound **5d**.

Structure-activity relationships of these acridones demonstrated that the electronic effect on the *N*-phenyl ring has some influence on the cytotoxic potency. For example, these derivatives (**5b**, **5d**, **5f**, **5h**, **5j**) with methoxy group on the ring have lower IC_{50} values than those corresponding derivatives (**5a**, **5c**, **5e**, **5g**, **5i**). These results are according to that reported by Gao and co-workers, whose studies revealed that compounds, which have more methoxy group on *N*-phenyl ring showed better activity against CCRF-CEM cells, and the compound with dimethoxy groups at C3 and C5 positions on the ring had the lowest IC_{50} at about 0.71 μM. On the other hand, a comparison of the substitute position on acridone ring demonstrated that a 4-substituted group (**5c**, **5d**, **5g**, **5h**) may have more significant improved antiproliferative activity than a 2-substituted group (**5e**, **5f**, **5i**, **5j**), and it showed the most potent inhibitory activity when the 4 position on the acridone was substituted by methoxy group. This result may be explained because of the dihedral angle between acridone ring and *N*-phenyl ring resulting from steric hindrance of 4-substituted group, and the different electronic effect. In addition, this trend was also observed by comparison of the two most potent compounds **5g** and **5h**; the latter with a 3′-mothoxy group showed a better activity. However, it remains to be further investigated how the change of the substitute on the *N*-phenyl ring influences the cytotoxic activity. In summary, the 4-substituted was found to play a very important role in the cytotoxic potency of these acridone derivatives.

Table 1. Structures and Cytotoxicity of Compounds 5a-5j Against Hep-G2

	R_1	R_2	IC_{50} (μM)
5a	H	H	19.15±1.13
5b	H	OCH_3	6.01±0.35
5c	4-CH_3	H	5.92±0.21
5d	4-CH_3	OCH_3	2.85±0.11
5e	2-CH_3	H	21.71±1.24
5f	2-CH_3	OCH_3	11.19±0.98
5g	4-OCH_3	H	2.58±0.15
5h	4-OCH_3	OCH_3	1.33±0.13
5i	2-OCH_3	H	17.20±1.7
5j	2-OCH_3	OCH_3	12.15±0.61
5-Fu			1.52±0.14

IC_{50} = 50% inhibitory concentration represents the mean ± S. D. from dose-response curves of at least three experiments.

4. THE INDUCTION OF APOPTOSIS IN HEP G2 CELLS BY COMPOUND 5H

In order to identify whether these acridone derivatives induced cell death in apoptotic mode, we observed com-

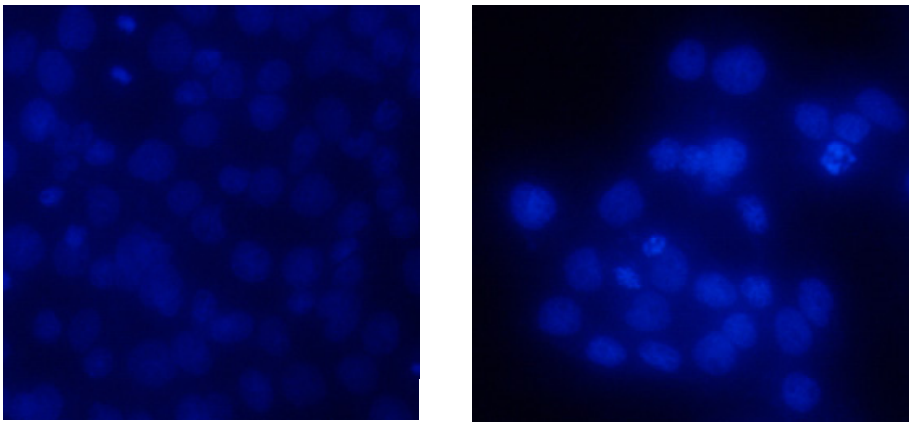

a **b**

Fig. (2). Fluorescent microscopic analysis of apoptotic cells. Cells stained with DAPI after treated with compound **5h** for 24 h. (**a**) control, (**b**) 2.50 μM.

pound **5h**-treated Hep G2 cells by staining with DAPI. The apoptotic nuclei were filled with condensed or fragmented chromatin, which showed enhanced fluorescence with DAPI staining. Distinguished apoptosis was seen in the cells treated with compound **5h**compared with the control group (Fig. **2**).

To further confirm that compound **5h** leads to apoptosis, Hep G2 cells were stained with annexin V-FITC and propidium iodide, and subsequently analyzed by flow cytometry. As shown in Fig. (**3**), a significant induction of apoptosis was shown by compound **5h** treatment. Compared to the control, cells treated with different concentration of compound **5h** for 24 h had an increase in the percentage of early apoptotic cells (Annexin V positive but PI negative) from 0.01% to 27.38%, and of late apoptotic cells (Annexin V and PI double-positive cells) from 0.20% to 16.88%. It is obvious, that as the concentration increased, the apoptosis rate gradient grew.

5. CONCLUSION

A series of acridones were synthesized and their antiproliferative activities against the human liver cancer cell line Hep G2 were evaluated. Some compounds displayed good cytotoxic activities and the SARs have also been studied. The consequences demonstrated that substitution at the 4 position of the acridone ring plays a very important role in the activity against Hep G2 cells. Among the compounds tested, compound **5h** exhibited the most potent activity in tumor growth inhibition (IC_{50}=1.5 μM). Through DAPI staining and Annexin V-FITC and PI staining for apoptosis, we have found the compound **6** induced cell death in apoptotic mode. Above all, compound **5h** would be a potential anticancer agent which deserves further research. More information regarding SAR and the mechanism of apoptosis induction are currently under way in our laboratory.

6. EXPERIMENTAL PROTOCOLS

6.1. Chemistry

All the NMR spectra were recorded on a Bruker DRX 500 or DPX 300 model Spectrometer in $CDCl_3$. Chemical shifts (δ) for 1H NMR spectra were reported in parts per million to residual solvent protons. Melting points were measured on a Boetius micro melting point apparatus. The ESI-MS spectra were recorded on a Mariner System 5304 Mass spectrometer. All chemicals and reagents used in current study were of analytical grade. TLC was running on the silica gel coated aluminum sheets (Silica Gel 60 GF254, E. Merk, Germany) and visualized in UV light (254 nm).

6.2. General Procedure for Compounds 5a-5j Preparations

To a mixture of *o*-chlorobenzoic acid (0.064 mol), corresponding aniline (0.064 mol), and copper powder (0.2 g) in 60 mL of DMF, dry K_2CO_3 (10 g) was slowly added and the contents were refluxed for 5 h. The mixture was poured into 1 L of hot water, and acidified. Precipitate formed was filtered, washed with hot water and collected. The crude acid was dissolved in aqueous sodium hydroxide solution, boiled in the presence of activated charcoal, and filtered. On acidification, light yellowish precipitate was obtained which was washed with hot water and recrystallized from aqueous methanol to give a light yellow solid **3** (yield 72-86 %).

3 (5 g) was taken in a flask to which was added 52 g of polyphosphoric acid. The reaction mixture was heated on oil-bath at 120 ^oC for 3 h with stirring. Appearance of yellow color indicated the completion of the reaction. Then, it was poured into 1 L of hot water, and made alkaline by liquor ammonia. The yellow precipitate formed was filtered, washed with hot water and collected. The sample of **4** was recrystallized from acetic acid (yield 71-85%).

Compound **4** (1 mmol), proportional benzyl chloride, and K_2CO_3 in 50 ml of dry DMF were stirred at 90–100 ^oC for 3–6 h. After the completion of reaction, the solution was added to a mixture of ice and H_2O, and the yellow solution was extracted with three 10-ml portions of AcOEt. The combined organic layers were washed with H_2O, dried (Na_2SO_4), filtered, evaporated, and recrystallized from AcOEt.

6.2.1. 10-benzylacridin-9(10H)-one (5a)

Yellow powder, yield: 71%. Mp: 180-181 ^oC. ^1H NMR (500 MHz, $CDCl_3$, δ ppm): 4.50 (s, 2H), 7.17 (d, 1H, J = 7.5

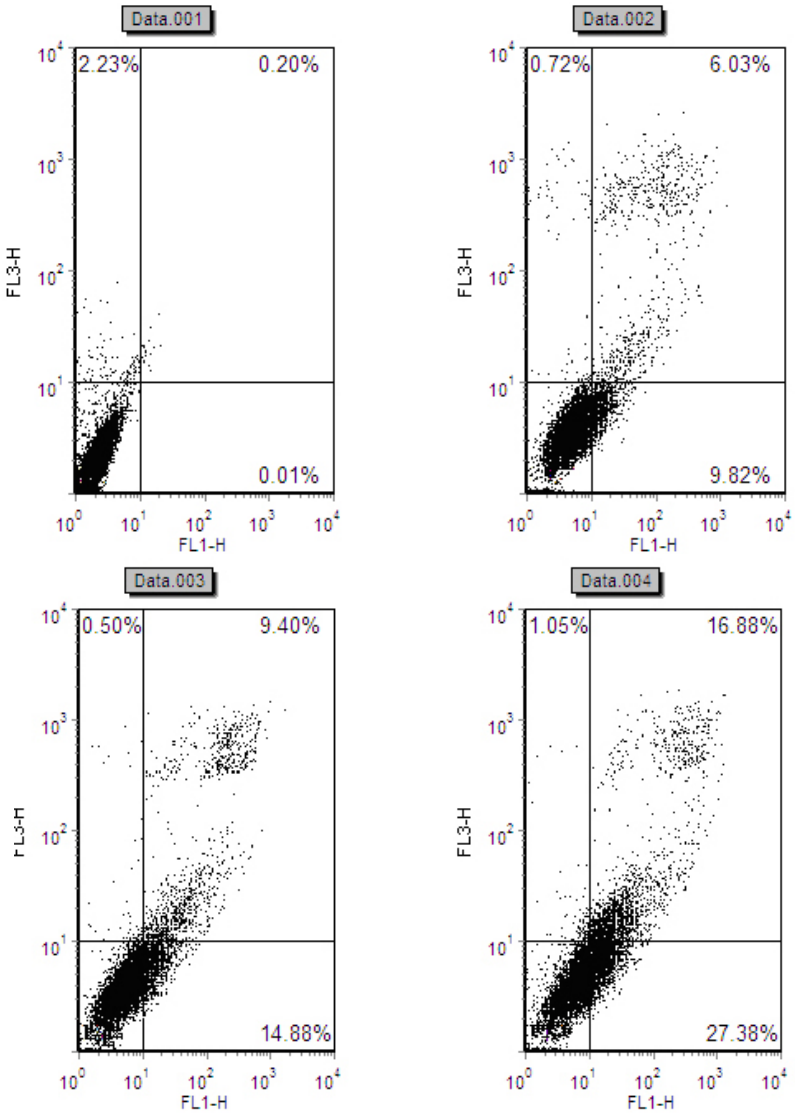

Fig. (3). Induction of apoptosis by compound **5h**. Flow cytometric analysis of annexin V-FITC and propidium iodide double stained cells. Cells were untreated or treated with different concentration of compound 5h for 24 h. Data represent the percentage of aopototic cells. (**a**) control, (**b**) 1.0 μM , (**c**) 2.0 μM , (**d**) 4.0 μM.

Hz), 7.23 (m, 1H), 7.31-7.44 (m, 8H), 7.65 (d, 1H, *J* = 8.5 Hz), 7.76 (t, 1H, *J* = 7.5 Hz), 8.41 (m, 1H). MS (ESI): 286.9 ($[M+H]^+$). Anal. Calcd for $C_{20}H_{15}NO$: C, 84.19; H, 5.30; N, 4.91. Found: C, 84.56; H, 5.31; N, 4.93.

6.2.2. 10-(3-methoxybenzyl)acridin-9(10H)-one (5b)

Yellow powder, yield: 73%. Mp: 211-212 °C. ^{1}H NMR (300 MHz, $CDCl_3$, δ ppm): 3.70 (s, 3H), 5.78 (s, 2H), 6.64 (d, 1H, *J* = 7.5 Hz), 6.81 (s, 1H), 6.85 (d, 1H, *J* = 8.0 Hz), 7.22 (t, 1H, *J* = 8.0 Hz), 7.35 (t, 2H, *J* = 7.5 Hz), 7.64 (d, 2H, *J* = 8.5 Hz), 7.77 (m, 2H), 8.38 (m, 2H). MS (ESI): 316.1 ($[M+H]^+$). Anal. Calcd for $C_{21}H_{17}NO_2$: C, 79.98; H, 5.43; N, 4.44. Found: C, 79.46; H, 5.41; N, 4.40.

6.2.3. 10-benzyl-4-methylacridin-9(10H)-one (5c)

Yellow powder, yield: 61%. Mp: 125-126 °C. ^{1}H NMR (500 MHz, $CDCl_3$, δ ppm): 2.61 (s, 3H), 5.65 (s, 2H), 7.03 (d, 2H, *J* = 7.5 Hz), 7.19 (m, 1H), 7.22-7.31 (m, 4H), 7.57 (d, 1H, *J* = 8.8 Hz), 7.64 (m, 2H), 8.20 (m, 2H). MS (ESI): 300.3 ($[M+H]^+$). Anal. Calcd for $C_{21}H_{17}NO$: C, 84.25; H, 5.72; N, 4.68. Found: C, 84.58; H, 5.71; N, 4.63.

6.2.4. 10-(3-methoxybenzyl)-4-methylacridin-9(10H)-one (5d)

Colorless crystal (petroleum ether/EtOAc, CCDC number: 804502), yield: 64%. Mp: 119-120 °C. ^{1}H NMR (300 MHz, $CDCl_3$, δ ppm): 2.61 (s, 3H), 3.74 (s, 2H), 5.61 (s, 2H), 6.59 (d, 1H, *J* = 8.0 Hz), 6.62 (s, 1H), 6.78 (m, 1H), 7.17 (t, 1H, *J* = 7.5 Hz), 7.21-7.29 (m, 2H),7.58 (d, 1H, *J* = 8.8 Hz), 7.64 (m, 2H), 8.20 (m, 2H). MS (ESI): 330.8 ($[M+H]^+$). Anal. Calcd for $C_{22}H_{19}NO_2$: C, 80.22; H, 5.81; N, 4.25. Found: C, 80.53; H, 5.85; N, 4.27.

6.2.5. 10-benzyl-2-methylacridin-9(10H)-one (5e)

Yellow powder, yield: 85%. Mp: 163-164 °C. ^{1}H NMR (500 MHz, $CDCl_3$, δ ppm): 2.46 (s, 3H), 5.59 (s, 2H), 7.20

(d, 2H, *J* = 7.0 Hz), 7.25-7.37 (m, 6H), 7.45 (dd, 1H, *J* = 2.0 Hz, 8.8 Hz), 7.62 (m, 1H), 8.39 (d, 1H, *J* = 2.0 Hz), 8.61 (m, 1H). MS (ESI): 300.1 ($[M+H]^+$). Anal. Calcd for $C_{21}H_{17}NO$: C, 84.25; H, 5.72; N, 4.68. Found: C, 84.71; H, 5.76; N, 4.71.

6.2.6. 10-(3-methoxybenzyl)-2-methylacridin-9(10H)-one (5f)

Yellow powder, yield: 80%. Mp: 156-158 °C. ^{1}H NMR (300 MHz, $CDCl_3$, δ ppm): 2.45 (s, 3H), 3.72 (s, 3H), 5.52 (s, 2H), 6.73–6.88 (m, 4H), 7.23–7.35 (m, 5H), 7.61 (m, 1H), 8.32 (m, 1H). MS (ESI): 330.0 ($[M+H]^+$). Anal. Calcd for $C_{22}H_{19}NO_2$: C, 80.22; H, 5.81; N, 4.25. Found: C, 80.46; H, 5.85; N, 4.20.

6.2.7. 10-benzyl-4-methoxyacridin-9(10H)-one (5g)

Amorphous crystal, yield: 63%. Mp: 145-146 °C. ^{1}H NMR (300 MHz, $CDCl_3$, δ ppm): 3.63 (s, 3H), 5.76 (s, 2H), 7.16 (m, 2H), 7.17 (m, 1H), 7.20-7.29 (m, 4H), 7.32 (m, 1H), 7.51 (d, 1H, *J* = 8.0 Hz), 7.68 (m, 1H), 7.96 (m, 1H), 8.28 (m, 1H). MS (ESI): 316.1 ($[M+H]^+$). Anal. Calcd for $C_{21}H_{17}NO_2$: C, 79.98; H, 5.43; N, 4.44. Found: 79.68; H, 5.45; N, 4.49.

6.2.8. 10-(3-methoxybenzyl)-4-methoxyacridin-9(10H)-one (5h)

Amorphous crystal, yield: 61%. Mp: 139-141 °C. ^{1}H NMR (300 MHz, $CDCl_3$, δ ppm): 3.59 (s, 3H), 3.81 (s, 3H), 5.61 (s, 2H), 6.80-6.95 (m, 3H), 7.17 (m, 1H), 7.21-7.29 (m, 3H), 7.37 (m, 1H), 7.57 (m, 1H), 8.19 (m, 1H), 8.50 (m, 1H). MS (ESI): 346.5 ($[M+H]^+$). Anal. Calcd for $C_{22}H_{19}NO_3$: C, 76.50; H, 5.54; N, 4.06. Found: C, 76.18; H, 5.53; N, 4.10.

6.2.9. 10-benzyl-2-methoxyacridin-9(10H)-one (5i)

Yellow powder, yield: 83%. Mp: 210-212 °C. ^{1}H NMR (300 MHz, $CDCl_3$, δ ppm): 3.90 (s, 3H), 5.52 (s, 2H), 7.20-7.29 (m, 4H), 7.32-7.59 (m, 6H), 7.96 (m, 1H), 8.49 (m, 1H). MS (ESI): 316.0 ($[M+H]^+$). Anal. Calcd for $C_{21}H_{17}NO_2$: C, 79.98; H, 5.43; N, 4.44. Found: C, 79.63; H, 5.49; N, 4.41.

6.2.10. 10-(3-methoxybenzyl)-2-methoxyacridin-9(10H)-one (5j)

Yellow powder, yield: 74%. Mp: 234-255 °C. ^{1}H NMR (300 MHz, $CDCl_3$, δ ppm): 3.75 (s, 3H), 3.92 (s, 3H), 5.51 (s, 2H), 6.73-6.89 (m, 4H), 7.17–7.26 (m, 4H), 7.62 (m, 1H), 7.96 (m, 1H), 8.49 (m, 1H). MS (ESI): 346.3 ($[M+H]^+$). Anal. Calcd for $C_{22}H_{19}NO_3$: C, 76.50; H, 5.54; N, 4.06. Found: C, 76.14; H, 5.58; N, 4.09.

6.3. Cytotoxicity Study on Hep G2 Cells

Hep G2 cells obtained from American Type Culture Collection (ATCC) were cultured in RPMI-1640 medium (GibcoBRL) with 10% (v/v) fetal bovine serum (FBS), 100 U/ml penicillin G and 100μg/ml streptomycin. Cells were incubated at 37°C in a humidified atmosphere of air/CO2 (95%: 5%). The antiproliferative activity was determined by using a standard (MTT)-based colorimetric assay (Sigma). Briefly, cell lines were seeded at a density of $7x10^3$ cells/well in 96-well microtiter plates (Costar). After 24 h, exponentially growing cells were exposed to the indicated compounds at final concentrations ranging from 0.1 to 100 μg/mL. After 48 h, cell survival was determined by the addition of MTT solution (10μL of 5 mg/mL MTT in PBS). After 4 h, 100 μL of 10% SDS (Sigma) in 0.01 N HCl was added, and the plates were incubated at 37 °C for a further 18 h; optical absorbance was measured at 570 nm on LX300 Epson Diagnostic microplate reader. Survival ratios are expressed in percentages with respect to untreated cells. IC_{50} values were determined from replicates of 6 wells from at least two independent experiments.

6.4. DAPI Staining Assay

Hep G2 cells were seeded in 6-well plates at a seeding density of 10^5 cells/ml. When all the cells were adhered, compound **5h** was added. After 24 h incubation, the cells were fixed with 4% paraformaldehyde for 20 minutes and permeabilized by incubation in 0.1% sodium citrate containing 0.1% Triton® X-100 (Sigma) for 2 minutes at 4°C, then labeled with DAPI (Sigma, 300 nM). After labeling, the apoptotic cells were visualized using a Nikon E800 (Nikon, Japan) microscope. The cells were considered to be apoptotic when they showed either fragmented or condensed nuclei. The apoptotic cells were defined morphologically by cytoplasmic and nuclear shrinkage and chromatin condensation or fragmentation [28].

6.5. Annexin-V/PI Double-Staining Assay

The Annexin V- FITC binding assay was performed by an Annexin V-FITC apoptosis detection kit (Nanjing KeyGen Biotech. Co. Ltd.) according to the manufacturer's protocol. The cells were seeded and treated with compound **5h** as for the DAPI staining assay. After 24 h incubation, the cells were trypsinized, washed in PBS and resuspended in binding buffer (10 mM Hepes/NaOH, pH 7.4, 140 mM NaCl, 2.5 mM CaCl2). The cells were incubated with Annexin V-FITC (100 ng/ml) in the dark for 10 min and 10 ml propidium iodide (PI) was added to each group before flow cytometric analysis. Positive Annexin V staining indicated apoptosis, while positive PI indicated necrosis. For each group, a minimum of 10,000 cells were counted. Data analysis was performed with standard Cell Quest software [29]. (FACSCA2BUR, Becton Dickinson, USA)

ACKNOWLEDGEMENTS

The work was supported by the Doctoral Fund (Project ZMF 08020066) of Changzhou University.

REFERENCES

[1] Bruix, J.; Boix, L.; Sala, M.; Llovet, J. M. Focus on hepatocellular carcinoma. *Cancer Cell,* **2004**, *5*, 215-219.

[2] Thorgeirsson, S. S.; Grisham, J. W. Molecular pathogenesis of human hepatocellular carcinoma. *Nat. Genet,* **2002**, *31*, 339-346.

[3] Farazi, P. A.; DePinho, R. A. Hepatocellular carcinoma pathogenesis: from genes to environment. *Nat Rev Cancer,* **2006**, *6*, 674-687.

[4] Parkin, D. M.; Bray, F.; Ferlay, J.; Pisani, P. Estimating the world cancer burden: Globocan 2000. *Int. J. Cancer,* **2001**, *94*, 153-156.

[5] Feo, F.; Frau, M.; Tomasi, M. L.; Brozzetti, S.; Pascale, R. M. Genetic and epigenetic control of molecular alterations in hepatocellular carcinoma. *Exp. Biol. Med.,* (Maywood) **2009**, *234*, 726-736.

[6] Sell, S. Cellular origin of hepatocellular carcinomas. *Semin. Cell Dev. Biol.*, **2002**, *13*, 419-424.

[7] Nesterenko, V.; Putt, K. S.; Hergenrother, P. J. Identification from a combinatorial library of a small molecule that selectively induces apoptosis in cancer cells. *J. Am. Chem. Soc.*, **2003**, *125*, 14672-14673.

[8] Zobel, K.; Wang, L.; Varfolomeev, E.; Franklin, M. C.; Elliott, L. O.; Wallweber, H. J. A.; Okawa, D. C.; Flygare, J. A.; Vucic, D.; Fairbrother, W. J.; Deshayes, K. Design, synthesis, and biological activity of a potent Smac mimetic that sensitizes cancer cells to apoptosis by antagonizing IAPs. *Acs. Chem. Biol.*, **2006**, *1*, 525-533.

[9] Fabregat, I.; Roncero, C.; Fernandez, M. Survival and apoptosis: a dysregulated balance in liver cancer. *Liver Int.*, **2007**, *27*, 155-162.

[10] Ding, G. Y.; Liu, F.; Yang, T.; Jiang, Y. Y.; Fu, H.; Zhao, Y. F. A novel kind of nitrogen heterocycle compound induces apoptosis of human chronic myelogenous leukemia K562 cells. *Bioorg. Med. Chem.*, **2006**, *14*, 3766-3774.

[11] Yang, J.; Jiang, Y. Y.; Liu, F.; Zhao, Y. F. Mitochondria-regulated death pathway mediates (DIPP-L-Leu)2-L-LysOCH3-induced K562 cells apoptosis. *Protein Peptide Lett.*, **2006**, *13*, 129-134.

[12] Van Heemst, D.; Den Reijer, P. M.; Westendorp, R. G. Ageing or cancer: a review on the role of caretakers and gatekeepers. *Eur. J. Cancer*, **2007**, *43*, 2144-2152.

[13] Prinz, H.; Ishii, Y.; Hirano, T.; Stoiber, T.; Gomez, J. A. C.; Schmidt, P.; Dussmann, H.; Burger, A. M.; Prehn, J. H. M.; Gunther, E. G.; Unger, E.; Umezawa, K. Novel benzylidene-9(10H)-anthracenones as highly active antimicrotubule agents. Synthesis, antiproliferative activity, and inhibition of tubulin polymerization. *J. Med. Chem.*, **2003**, *46*, 3382-3394.

[14] Demeunynck, M.; Charmantray, F.; Martelli, A. Interest of acridine derivatives in the anticancer chemotherapy. *Curr. Pharm. Des.*, **2001**, *7*, 1703-1724.

[15] Belmont, P.; Bosson, J; Godet, T.; Tiano, M. Acridine and acridone derivatives, anticancer properties and synthetic methods: where are we now? *Anti-Cancer Agents Med. Chem.*, **2007**, *7*, 139-169.

[16] Goodell, J. R.; Ougolkov, A. R.; Hiasa, H.; Kaur, H.; Remmel, R.; Billadeau, D. D.; Ferguson, D. M. Acridine-based agents with topoisomerase II activity inhibit pancreatic cancer cell proliferation and induce apoptosis. *J. Med. Chem.*, **2008**, *51*, 179-182.

[17] Kawaii, S.; Tomono, Y.; Katase, E.; Ogawa, K.; Yano, M.; Takemura, Y.; Ju-ichi, M.; Ito, C.; Furukawa, H. The antiproliferative effect of acridone alkaloids on several cancer cell lines. *J. Nat. Prod.*, **1999**, *62*, 587-589.

[18] Koba, M.; Baczek T. Chemometric Evaluation of the Significance of Molecular Structural Descriptors on Binding of Acridinone Derivatives to DNA. *Letters in Drug Design & Discovery*, **2010**, *7*, 494-499.

[19] Winter, R. W.; Kelly, J. X.; Smilkstein, M. J.; Dodean, R.; Bagby, G. C.; Rathbun, R. K.; Levin, J. I.; Hinrichs, D.; Riscoe, M. K. Evaluation and lead optimization of anti-malarial acridones. *Exp. Parasitol.*, **2006**, *114*, 47-56.

[20] Dheyongera, J. P.; Geldenhuya, W. J.; Dekker, T. G.; Matsabisa, M. G.; Van der Schyf, C. J. Antimalarial activity of thioacridone compounds related to the acronycine alkaloid. *Bioorg. Med. Chem.*, **2005**, *13*, 1653-1569.

[21] Di Giorgio, C.; Shimi, K.; Boyer, G.; Delmas, F.; Galy, J. P. Synthesis and antileishmanial activity of 6-mono-substituted and 3,6-di-substituted acridines obtained by acylation of proflavine. *Eur. J. Med. Chem.*, **2007**, *42*, 1277-1284.

[22] Goodell, J. R.; Madhok, A. A.; Hiasa, H.; Ferguson, D. M. Synthesis and evaluation of acridine- and acridone-based anti-herpes agents with topoisomerase activity. *Bioorg. Med. Chem.*, **2006**, *14*, 5467-5480.

[23] Gao, C.; Jiang, Y.; Tan, C.; Zu, X.; Liu, H.; Cao, D. Synthesis and potent antileukemic activities of 10-benzyl-9(10H)-acridinones. *Bioorg. Med. Chem.*, **2008**, *16*, 8670-8675.

[24] Putic, A.; Stecher, L.; Prinz, H.; Müller, K. Structure-activity relationship studies of acridones as potential antipsoriatic agents. 2. Synthesis and antiproliferative activity of 10-substituted hydroxy-10*H*-acridin-9-ones against human keratinocyte growth. *Eur. J. Med. Chem.*, **2010**, *45*, 5345-5352.

[25] Stankiewicz-Drogon, A.; Palchykovska, L. G.; Kostina, V. G.; Alexeeva, I. V.; Shved, A. D.; Boguszewska-Chachulska, A. M. New acridone-4-carboxylic acid derivatives as potential inhibitors of hepatitis C virus infection. *Bioorg. Med. Chem.*, **2008**, *16*, 8846-8852.

[26] Galy, A. M.; Barbe, J. Alkylation en catalyse par transfert de phase d'une série d'acridanone-9 substitutées: compétition entre *O* – et *N*-alkylation. *J. Heterocyclic Chem.*, **1982**, *19*, 503-507.

[27] Blanchard, C.; Montginoul, C.; Torreilles, E.; Giral, L. Alkylation et acylation d'acridanone-9. *J. Heterocyclic Chem.*, **1981**, *18*, 841-843.

[28] Ling, Y.; Lu, N.; Gao, Y.; Chen, Y.; Wang, S.; Yang, Y.; Guo, Q. Endostar Induces Apoptotic Effects in HUVECs through Activation of Caspase-3 and Decrease of Bcl-2. *Anticancer Res.*, **2009**, *29*, 411-417.

[29] Wu, S. J.; Ng, L. T.; Chen, C. H.; Lin, D. L.; Wang, S. S.; Lin, C. C. Antihepatoma activity of Physalis angulata and P. peruviana extracts and their effects on apoptosis in human Hep G2 cells. *Life Sci.*, **2004**, *74*, 2061-2073.